DOI: 10.1002/anie.201204776

Tubular Assemblies

Solution-Phase and Magnetic Approach towards Understanding Iron Gall Ink-like Nanoassemblies**

Harshita Kumari, Steven R. Kline, Cindi L. Dennis,* Andrew V. Mossine, Rick L. Paul, Carol A. Deakyne,* and Jerry L. Atwood**

The degradative oxidation of Leonardo da Vinci's oeuvre, the works of Galileo, and many other imperiled ancient manuscripts is, ironically, catalyzed by the very ink that was used to write them.[1] Historical artifacts such as these are characterized by the extensive use of "iron gall ink", an ink commonly used prior to the twentieth century. Regardless of the specific composition, iron gall inks are complexes of various polyphenolic gallic acids, a class of tannins, and ferric/ferrous ions, along with other agents such as gypsum and gum arabic. In the interest of preserving such invaluable works of ancient prose, Fe complexes with polyphenolic compounds, such as gallic acid, catechin, ellagic acid and pyrogallol, have been extensively studied by IR, ESR, NMR, XANES and Mössbauer spectroscopy.[2] However, structural elucidation of these complexes has proven difficult. Our interest in this field stems from the difficulty in characterizing similar Fe-polyphenolic complexes, namely the complexes with the bowl-shaped pyrogallol[4]arenes (PgC_n, n = alkyl chain length). Compared to other PgC-transition metal capsular entities, which have been thoroughly studied and characterized by XRD, the structure of the PgC_nFe complexes has largely remained a mystery, much like that of the chemically similar gall inks.[3] Herein, we present a new approach towards the characterization of these unique complexes through the combination of solid-state magnetic and in situ neutron scattering methods.

In our previous studies, solid-state properties aided our understanding of solution-phase behavior.[4] For example, solid-state PgC_nM entities (M = Zn, Cu, Ni, Co) are spherical, and our small-angle neutron scattering (SANS) experiments indicate that they retain that architecture when dissolved in non-polar solvents.[5] In contrast, solid-state PgC_4Ga and PgC_4GaZn entities have rugby-ball and spherical shapes, respectively, which convert to toroids of different metric dimensions in solution.[6] Thus, SANS allows differentiation between architectures of similar metric dimensions and between varying metric dimensions of similar architectures.[5a,6]

The current study addresses our three-fold interest in investigating solution structures of magnetically interesting self-assembled frameworks, obtaining solid-state insight from solution-phase studies and exploring the parameters that direct self-assembly. Specifically, the stability, elemental ratios and magnetic properties of Fe-containing *C*-alkylpyrogallol[4]arene (PgC_nFe) nanoassemblies were examined.

PgC_1Fe or PgC_3Fe was synthesized by mixing 4 equiv of $Fe(NO_3)_3$ with 1 equiv of PgC_n and 14 equiv of C_5H_5N (Py) in a variety of solvent systems. The blue-black precipitates obtained could not be crystallized; thus, structural studies were conducted using SANS. The solid-state magnetic behavior of these entities was investigated using a SQUID magnetometer. The composition of these nanoframeworks was measured with prompt gamma activation analysis (PGAA).

The PGAA results for solid-state PgC_1Fe and PgC_3Fe reveal C:Fe ratios of 27.8:1 and 28.5:1 and C:N ratios of 28.1:1 and 29.2:1, respectively (see Supporting Information). The 1:1 ratio between Fe and C_5H_5N-derived nitrogen agrees with the metal:Py ratios typically found in metal-seamed pyrogallol[4]arene dimeric host capsules.[5b,c] However, in contrast to the typical capsular metal:PgC_n ratio of 4:1, the Fe:PgC_n ratio was unexpectedly deduced to be 1.3:1.[5a] This ratio also differs from those for the tubular and dimeric PgC_1⊂ferrocene (PgC_1⊂Fc) hydrogen-bonded inclusion complexes, for which the Fc:PgC_1 ratios are 1:3 and 1:2, respectively.[4c,7]

In the SANS study, the [D_6]DMSO-solubilized PgC_1Fe (3% mass fraction) was measured on the NG7 30 m SANS instrument at the NIST Center for Neutron Research (NCNR) in Gaithersburg, MD[8] and analyzed with IGOR Pro.[9] The scattering length density (SLD) of PgC_1Fe was calculated at the molar ratio of 1:1.3:1.3 (PgC_1:Fe:Py) obtained from the PGAA results, and the scattering data was fitted to spherical,[10] cylindrical[11] and ellipsoidal models.[12] The data analysis revealed distinct structural differences between previously investigated metal-seamed spherical[4a,c] nanoassemblies and the Fe-containing pyrogallol[4]arene nanoassemblies (Figure 1). The scattering for PgC_1Fe was higher at low scattering angles (q) and fitted

[*] Dr. H. Kumari, A. V. Mossine, Prof. C. A. Deakyne, Prof. J. L. Atwood
Department of Chemistry, University of Missouri-Columbia
601 S. College Avenue, Columbia, MO 65211 (USA)
E-mail: deakynec@missouri.edu
atwoodj@missouri.edu
Dr. S. R. Kline
NIST Center for Neutron Research
National Institute of Standards and Technology
100 Bureau Drive, Gaithersburg, MD 20899 (USA)
E-mail: steven.kline@nist.gov
Dr. C. L. Dennis, Dr. R. L. Paul
Material Measurement Laboratory
National Institute of Standards and Technology
100 Bureau Drive, Gaithersburg, MD 20899 (USA)
E-mail: cindi.dennis@nist.gov

[**] We thank NSF for support of this work (J.L.A.) and NIBIB for training grant T21 EB004822 (A.V.M.). This work utilized facilities supported in part by the NSF under Agreement No. DMR-0944772 (S.R.K.).

Supporting information for this article is available on the WWW under http://dx.doi.org/10.1002/anie.201204776.

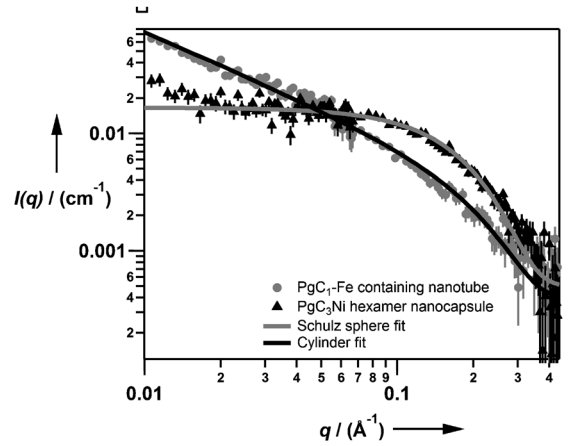

Figure 1. SANS data of PgC_1Fe tube (gray circles) and PgC_3Ni sphere (black triangles). Error bars on SANS data represent one standard deviation.

best to a cylindrical model. This is the first example of a PgC-based tubular architecture in solution. In our earlier SANS studies of a variety of H-bonded tubular assemblies, the tubes rearranged to dimers in solution, which suggests retention of Fe in the tubular framework of PgC_1Fe.[4c,7b,13]

The radius (R) and length (L) of the cylinder for PgC_1Fe were found to be ca. 7 Å and 124 Å, respectively (Figure 2). Due to the range of scattering angles chosen initially, it was

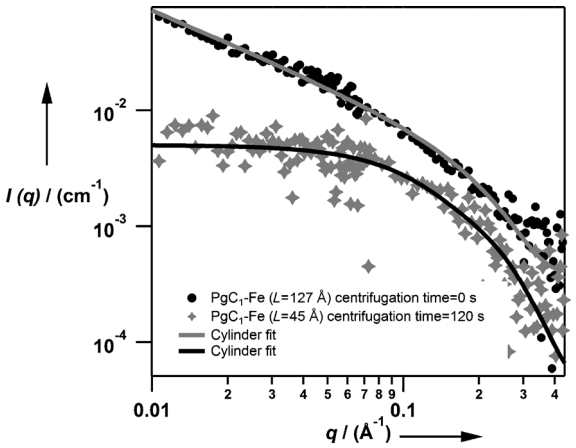

Figure 2. SANS cylindrical fits for the PgC_1Fe nanotubes (in DMSO) with varying chain lengths (black circles: $L = 127$ Å; gray diamonds: $L = 45$ Å) (see Supporting Information).

difficult to resolve the length parameter to very small error bars at low q values. As this was the case, we modified the experiment in two ways: a) the measurements were extended to lower scattering angles; and b) the sample was centrifuged (1 min) to ensure no precipitation occurred. The modified SANS experiments yielded cylindrical fitting parameters with improved statistics, confirming the tubular shape of PgC_1Fe. R remained at 7 Å but L decreased to 45 Å, suggesting that centrifugation time is a key factor in controlling the length of the nanotubular entity (Figure 2). This factor was further investigated by varying the centrifugation time from 0 to 2 min. Repeated data sets yielded a consistent radius of 7 Å and consistent lengths of 45 Å after 1 min and 27 Å after 2 min (Supporting Information).

The nature of the solvent and the addition of HNO_3 were also studied as possible independent factors controlling the geometry of PgC_1Fe in solution. Changing the solvent from DMSO to methanol did not affect the stability of the nanotubular framework. Specifically, the cylinder model gave similar dimensions of $R \approx 7$ Å and $L \approx 27$ Å. Hence, the effect of HNO_3 addition was tested only in methanol.

For the HNO_3 studies, the solution-phase PgC_1Fe moiety (ca. 10^{-3} mol L^{-1}) was produced from starting materials rather than by dissolving the pre-synthesized product in solvent. The lower concentration was used to avoid precipitation, and samples were allowed to stand for a day to equilibrate prior to SANS measurements. The molar ratio of Fe to PgC_1 was held constant at 4:1 but the molar ratio of C_5H_5N to HNO_3 was varied from 1:1, 1:0.8, 1:0.6, 1:0.4, 1:0.2 and 1:0 (control). The corresponding $PgC:C_5H_5N$ ratios thus ranged from 1:0 to 1:20 in increments of 4, assuming that pyridine is converted to pyridinium nitrate. Note that a 1:14 molar ratio of PgC:Py is typically used in the construction of nanocapsular arrangements.[5a]

For the samples with $Py:HNO_3$ molar ratios of 1:0 and 1:0.2, the scattering data fitted best to cylinders of $R = 6.5$–7.0 Å and $L = 24.0$–25.0 Å (Supporting Information).[11] Note the similarity in dimensions to the cylinders obtained in the DMSO and methanol solvent studies. The cylindrical fits for the samples with molar ratios of 1:0.4, 1:0.6, 1:0.8 and 1:1 showed increasingly shorter cylinder lengths and poorer statistics as the amount of acid was increased. Consistent with this trend, the data for these samples fit best to a spherical model, indicating a transition in architecture with the loss of C_5H_5N. Interestingly, hexamers form at ratios of 1:0.4, 1:0.6 and 1:0.8 but dimers form at a ratio of 1:1. An analogous change in morphology from tube to sphere has been observed for metalated *p*-sulfonated calix[4]arene assemblies.[14]

For the PgC_1 hexamers obtained in the current study $R \approx 9.8$ Å, consistent with $R \approx 10$ Å obtained previously for PgC_3M hexamers.[5a] In contrast, the ca. 8 Å radius of the PgC_1 dimer is about 1 Å larger than was found for PgC_3M dimers,[5a] suggesting that in the absence of deprotonation of the PgC upper rim hydroxy groups, an extended H-bonded dimer is assembled (Supporting Information). Since, to our knowledge, H-bonded hexamers have not been observed in methanol, these data sets suggest formation of metal-seamed hexameric nanocapsules. Thus, excess C_5H_5N appears to be required to form the Fe-containing tubes but not the Fe-containing hexamers.

Following the solution-phase studies, the solid-state magnetic behavior of PgC_1Fe was investigated. We performed magnetic moment (M) vs. magnetic field ($\mu_0 H$) measurements at 5 K and 50 K and M vs. temperature (T) measurements at 1.6 kA m^{-1}. A ferromagnet, such as clumps of Fe, should exhibit a coercivity. However, the hysteresis curves at both 5 K and 50 K reveal the paramagnetic behavior of PgC_1Fe (Figure 3) and no coercivity (within instrument resolution). As is common for paramagnets, the sample

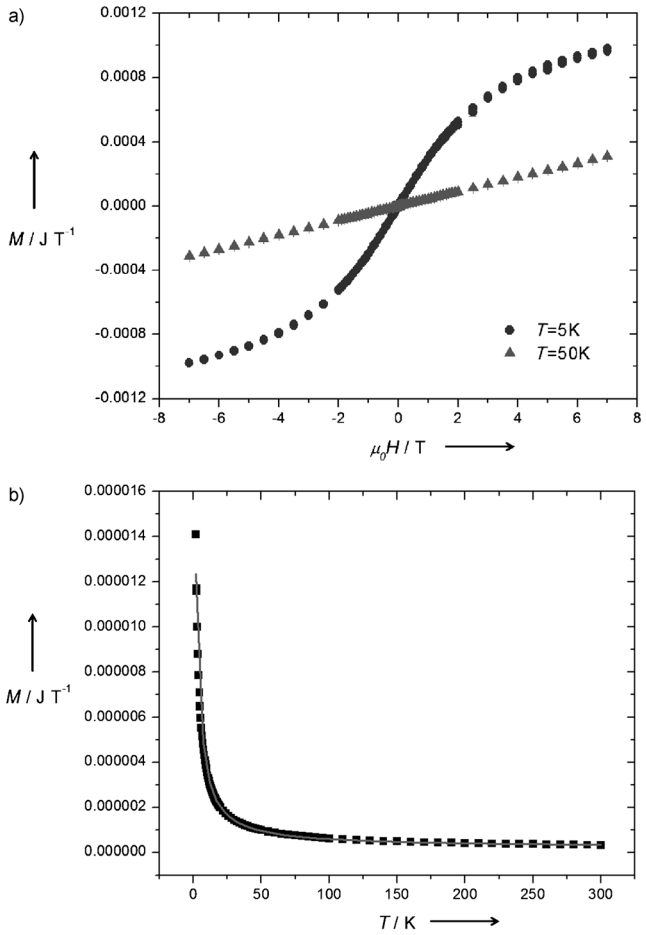

Figure 3. a) M vs. $\mu_0 H$ curve and b) M vs. T curve of PgC_1Fe nanoassembly. Fitting parameters for the M vs. T data: $\chi^2/$ DoF = 29050.62164; $R^2 = 0.99762$; $H = 3.8169 \times 10^{-5} \pm 1 \times 10^{-9}$; $T_c = -1.14 \pm 0.01$; gamma = 1 ± 0; $C = 2.1096 \times 10^{-7} \pm 2 \times 10^{-11}$.

does not completely saturate even at 5 K under 7 T. The paramagnetic behavior of PgC_1Fe is similar to that observed for PgC_3Ni dimers and hexamers or Fc-enclosed tubes and dimers.[4c,5b,7,15]

M vs. $\mu_0 H$ data at 5 K (Figure 3) was fitted to the quantum mechanical (QM) paramagnetic Equation (1).

$$M = Nm \tanh\left(\frac{gmJ\mu_0 H}{k_B T}\right) \quad (1)$$

Here g is the spectroscopic splitting factor ($g \equiv 2$), N is the number of atoms, T is the temperature, $\mu_0 H$ is the applied magnetic field in Tesla, M is the total magnetic moment, m is the magnetic moment per atom, k_B is Boltzmann's constant, and J is the spin angular moment ($J \equiv 1/2$). The QM fit for PgC_1Fe reveals 2.35 ± 0.01 μ_B per Fe atom and a total of 4.5×10^{19} Fe atoms. Interestingly, this magnetic moment is higher than those observed for the $PgC_1{\subset}Fc$ dimer (2.30 μ_B/Fe atom), $PgC_1{\subset}Fc$ tube (2.16 μ_B/Fe atom), PgC_3Ni hexamer (1.68 μ_B/Ni atom), and PgC_3Ni dimer (1.65 μ_B/Ni atom). The difference in magnetic moment per Fe atom between the Fc-enclosed pyrogallol[4]arene complexes and PgC_1Fe can be attributed to differences in structure and/or the position of the metal atoms. On the other hand, the inherent magnetic differences between Fe and Ni account for the noticeable difference in μ_B between the PgC_1Fe and PgC_3Ni nanoassemblies.

The M vs. T data for PgC_1Fe (Figure 3) was fitted to the Curie–Weiss law using Equation (2).

$$M = \frac{A}{(T - T_{int})^{\gamma}} + C \quad (2)$$

Here T_{int} is the interaction temperature, A and C are constants, and γ is the critical exponent ($\gamma \equiv 1$). Any deviation from an ideal non-interacting paramagnet takes the form of a negative or positive interaction "temperature", characteristic of an antiferromagnetic or ferromagnetic interaction, respectively, between the metal centers. The M vs. $\mu_0 H$ and M vs. T curves for PgC_1Fe support paramagnetic behavior; however, the Curie–Weiss fit yields a small deviation with a negative $T_{int} = -1.14$ K. The observed antiferromagnetic alignment originates from weak dipolar interactions among adjacent Fe atoms. The fits for both the PgC_3Ni nanocapsule and $PgC_1{\subset}Fc$ nanotube revealed similar deviations from ideal paramagnetism and gave T_{int} values of -2.3 K and -0.5 K, respectively.[4c,5b,7,15] However, although the moment of each Fe center is higher than that of Ni, the T_{int} and, therefore, the dipolar interactions are affected by the distance between the metal centers. That is, the magnitude of the dipolar interaction or direct exchange coupling between metal atoms is dependent upon the length scales and the overlap of wavefunctions.

The guest Fe atoms in a given $PgC_1{\subset}Fc$ tube are about 6 Å apart, whereas adjacent Ni atoms on the surface of a given dimer/hexamer host are about 4 Å apart.[4c,5b,7,15] The distance between the guest Fe atoms of two adjacent $PgC_1{\subset}Fc$ dimers/tubes is about 12 Å/21 Å. The combined magnetic and structural studies of these $PgC_1{\subset}Fc$ entities clearly indicate that encapsulation of metal atoms significantly diminishes the dipolar attraction between them.[4c] That the T_{int} of PgC_1Fe (-1.14 K) is intermediate between those of $PgC_1{\subset}Fc$ (-0.47 K) and PgC_3Ni (-2.26 K) suggests a structural analogy among the pyrogallol[4]arene tubular and capsular scaffolds. The absence of any coercivity and the similar PgC_1Fe and PgC_3Ni T_{int} values show the absence of free Fe and support the presence of Fe in a tubular framework. If the framework were spherical we would expect a more negative T_{int} for PgC_1Fe than for PgC_3Ni because the distance between the metal centers should be similar for the two spheres but the magnetic moment per atom is higher for Fe than for Ni.[4c,5b,7a,b,15]

At spacings less than 1 nm, the wavefunctions of metal atoms can overlap to yield direct exchange coupling; at larger distances the wavefunctions cease to overlap, resulting in a magnetic interaction that originates from only the dipolar fields produced by each moment (metal center). The low T_{int} of PgC_1Fe and the low PgC_1:Fe ratio obtained from PGAA thus suggest a spiral or canted arrangement of Fe metal centers in the tubular framework (Figure 4).

Solid-state analyses often aid in our understanding of solution-phase behavior;[4] however, the reverse process is not

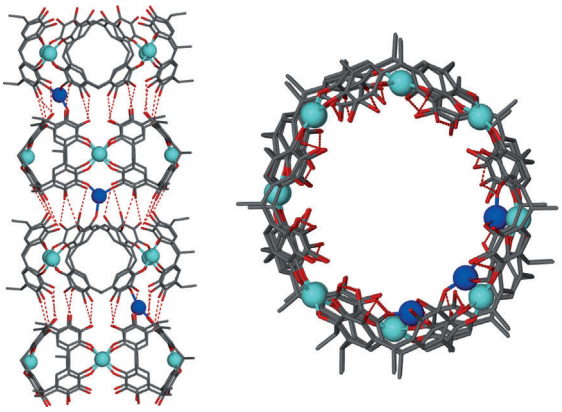

Figure 4. Proposed model of the PgC_1Fe framework. Front view (left) and top view (right). Gray C, red O, turquoise Fe within a PgC, blue Fe between two PgC.

generally implemented. In this work, the structural information obtained from the solution-phase study of an Fe-containing PgC_1 assembly aided in interpreting the magnetic properties of the solid-state assembly. PgC_1Fe is the first example of a metal-containing pyrogallol[4]arene-based tube in solution. The magnetic properties of solid-state PgC_1Fe are also consistent with a tubular architecture. That the Fe atoms are in the framework of the tube is supported by the following: a) H-bonded *C*-alkylpyrogallol[4]arene tubes are not stable in solution; b) the magnetic moment per Fe atom is much weaker than that of free Fe salts; and c) the PGAA and magnetic behavior of PgC_1Fe are similar to those of other metal-seamed pyrogallol[4]arene nanocapsules. The shape of the nanoassembly in solution was found to be controlled by C_5H_5N concentration; the length of the tubular assembly was found to be controlled by centrifugation time. It is likely that combined investigations of solution-phase properties and magnetic behavior will prove beneficial in characterizing more species that are difficult to crystallize, such as iron gall inks and the still relatively unexplored tubular nanoassemblies.

Received: June 19, 2012
Published online: August 13, 2012

Keywords: iron · magnetic properties · pyrogallol[4]arenes · small-angle neutron scattering (SANS) · supramolecular chemistry

[1] a) V. Rouchon, M. Duranton, C. Burgaud, E. Pellizzi, B. Lavédrine, K. Janssens, W. de Nolf, G. Nuyts, F. Vanmeert, K. Hellemans, *Anal. Chem.* **2011**, *83*, 2589–2597; b) J. Kolar, A. Stolfa, M. Strlic, M. Pompe, B. Pihlar, M. Budnar, J. Simcic, B. Reissland, *Anal. Chim. Acta* **2006**, *555*, 167–174.

[2] a) S. N. Podyachev, S. N. Sudakova, V. V. Syakaev, N. E. Burmakina, R. R. Shagidullin, V. I. Morozov, L. V. Avvakumova, A. I. Konovalov, *Russ. Chem. Bull.* **2010**, *58*, 80–88; b) J. A. Jaén, L. González, A. Vargas, G. Olave, *Hyperfine Interact.* **2003**, *148/149*, 227–235; c) I. Arčon, J. Kolar, A. Kodre, D. Hanžel, M. Strlič, *X-Ray Spectrom.* **2007**, *36*, 199–205; d) C. Burgaud, V. Rouchon, P. Refait, A. Wattiaux, *Appl. Phys. A* **2008**, *92*, 257–262; e) M. J. Hynes, M. O. Coinceanainn, *J. Inorg. Biochem.* **2001**, *85*, 131–142; f) C. Burgaud, V. Rouchon, A. Wattiaux, J. Bleton, R. Sabot, P. Refait, *J. Electroanal. Chem.* **2010**, *650*, 16–23.

[3] S. J. Dalgarno, N. P. Power, J. L. Atwood, *Coord. Chem. Rev.* **2008**, *252*, 825–841.

[4] a) H. Kumari, S. R. Kline, N. J. Schuster, J. L. Atwood, *Chem. Commun.* **2011**, *47*, 12298; b) H. Kumari, S. R. Kline, N. J. Schuster, C. L. Barnes, J. L. Atwood, *J. Am. Chem. Soc.* **2011**, *133*, 18102–18105.

[5] a) H. Kumari, A. V. Mossine, S. R. Kline, C. L. Dennis, D. A. Fowler, S. J. Teat, C. L. Barnes, C. A. Deakyne, J. L. Atwood, *Angew. Chem.* **2012**, *124*, 1481–1483; *Angew. Chem. Int. Ed.* **2012**, *51*, 1452–1454; b) J. L. Atwood, E. K. Brechin, S. J. Dalgarno, R. Inglis, L. F. Jones, A. Mossine, M. J. Paterson, N. P. Power, S. J. Teat, *Chem. Commun.* **2010**, *46*, 3484–3486; c) N. P. Power, S. J. Dalgarno, J. L. Atwood, *New J. Chem.* **2007**, *31*, 17–20.

[6] H. Kumari, S. R. Kline, W. Wycoff, R. L. Paul, A. V. Mossine, C. A. Deakyne, J. L. Atwood, *Angew. Chem.* **2012**, *124*, 5176–5181; *Angew. Chem. Int. Ed.* **2012**, *51*, 5086–5091.

[7] a) A. V. Mossine, H. Kumari, D. A. Fowler, A. K. Maerz, S. R. Kline, C. L. Barnes, J. L. Atwood, *Isr. J. Chem.* **2011**, *51*, 840–842; b) A. V. Mossine, H. Kumari, D. A. Fowler, A. Shih, S. R. Kline, C. L. Barnes, J. L. Atwood, *Chem. Eur. J.* **2012**, 18, 10258–10260.

[8] C. J. Glinka, J. G. Barker, B. Hammouda, S. Krueger, J. J. Moyer, W. J. Orts, *J. Appl. Crystallogr.* **1998**, *31*, 430–445.

[9] S. R. Kline, *J. Appl. Crystallogr.* **2006**, *39*, 895–900.

[10] a) G. V. Schulz, *Z. Phys. Chem. B* **1939**, *43*, 25–46; b) M. Kotlarchyk, S. H. Chen, *J. Chem. Phys.* **1983**, *79*, 2461–2469.

[11] A. Guinier, G. Fournet, *Small-Angle Scattering of X-rays*, Wiley, New York, **1955**, p. 268.

[12] D. I. Svergun, L. A. Feigin, *X-ray and Neutron Low-Angle Scattering*, Plenum, New York, **1986**, p. 278.

[13] a) "Solution, Magnetic and Insulin Encapsulation Study of Metal-seamed Organic Nanocaspules": H. Kumari, Ph.D. Thesis, University of Missouri-Columbia (Columbia), April 2011; b) H. Kumari, S. R. Kline, W. Wycoff, J. L. Atwood, *Small* **2012**, DOI: 10.1002.smll.201201384.

[14] G. W. Orr, L. J. Barbour, J. L. Atwood, *Science* **1999**, *285*, 1049–1052.

[15] H. Kumari, C. L. Dennis, A. V. Mossine, C. A. Deakyne, J. L. Atwood, *ACS Nano* **2012**, *6*, 272–275.

